Biomedical Optics EXPRESS

In vivo adaptive optics microvascular imaging in diabetic patients without clinically severe diabetic retinopathy

Stephen A. Burns,[1] Ann E. Elsner,[1,*] Toco Y. Chui,[1] Dean A. VanNasdale, Jr.,[1] Christopher A. Clark,[1] Thomas J Gast,[1] Victor E. Malinovsky,[1] and Anh-Danh T. Phan[2]

[1]*School of Optometry, Indiana University, 800 E. Atwater Ave, Bloomington, IN, 47405, USA*
[2]*Eugene and Marilyn Glick Eye Institute, Department of Ophthalmology, Indiana University School of Medicine, 1160 West Michigan Street, Indianapolis, IN 46202, USA*
** aeelsner@indiana.edu*

Abstract: We used a confocal adaptive optics scanning laser ophthalmoscope (AOSLO) to image the retina of subjects with non-proliferative diabetic retinopathy (NPDR). To improve visualization of different retinal features, the size and alignment of the confocal aperture were varied. The inner retinal layers contained clearly visualized retinal vessels. In diabetic subjects there was extensive capillary remodeling despite the subjects having only mild or moderate NPDR. Details of the retinal microvasculature were readily imaged with a larger confocal aperture. Hard exudates were observed with the AOSLO in all imaging modes. Photoreceptor layer images showed regions of bright cones and dark areas, corresponding in location to overlying vascular abnormalities and retinal edema. Clinically undetected intraretinal vessel remodeling and varying blood flow patterns were found. Perifoveal capillary diameters were larger in the diabetic subjects ($p<0.01$), and small arteriolar walls were thickened, based on wall to lumen measurements ($p<.05$). The results suggest that existing clinical classifications based on lower magnification clinical assessment may not adequately measure key vascular differences among individuals with NPDR.

OCIS codes: (170.3880) Medical and biological imaging; (170.4460) Ophthalmic optics and devices; (170.4470) Ophthalmology.

References and links

1. J. Liang, D. R. Williams, and D. T. Miller, "Supernormal vision and high-resolution retinal imaging through adaptive optics," J. Opt. Soc. Am. A **14**(11), 2884–2892 (1997).
2. A. Roorda, A. B. Metha, P. Lennie, and D. R. Williams, "Packing arrangement of the three cone classes in primate retina," Vision Res. **41**(10-11), 1291–1306 (2001).
3. J. Carroll, M. Neitz, H. Hofer, J. Neitz, and D. R. Williams, "Functional photoreceptor loss revealed with adaptive optics: An alternate cause of color blindness," Proc. Natl. Acad. Sci. U.S.A. **101**(22), 8461–8466 (2004).
4. S. S. Choi, N. Doble, J. L. Hardy, S. M. Jones, J. L. Keltner, S. S. Olivier, and J. S. Werner, "In vivo imaging of the photoreceptor mosaic in retinal dystrophies and correlations with visual function," Invest. Ophthalmol. Vis. Sci. **47**(5), 2080–2092 (2006).
5. R. S. Jonnal, J. Rha, Y. Zhang, B. Cense, W. H. Gao, and D. T. Miller, "In vivo functional imaging of human cone photoreceptors," Opt. Express **15**(24), 16141–16160 (2007).
6. T. Y. P. Chui, H. X. Song, and S. A. Burns, "Adaptive-optics imaging of human cone photoreceptor distribution," J. Opt. Soc. Am. A **25**(12), 3021–3029 (2008).
7. E. A. Rossi and A. Roorda, "The relationship between visual resolution and cone spacing in the human fovea," Nat. Neurosci. **13**(2), 156–157 (2010).
8. A. Dubra, Y. Sulai, J. L. Norris, R. F. Cooper, A. M. Dubis, D. R. Williams, and J. Carroll, "Noninvasive imaging of the human rod photoreceptor mosaic using a confocal adaptive optics scanning ophthalmoscope," Biomed. Opt. Express **2**(7), 1864–1876 (2011).

#200935 - $15.00 USD Received 15 Jan 2014; revised 15 Jan 2014; accepted 21 Feb 2014; published 27 Feb 2014

9. H. Song, T. Y. Chui, Z. Zhong, A. E. Elsner, and S. A. Burns, "Variation of cone photoreceptor packing density with retinal eccentricity and age," Invest. Ophthalmol. Vis. Sci. **52**(10), 7376–7384 (2011).
10. A. Roorda, Y. H. Zhang, and J. L. Duncan, "High-resolution in vivo imaging of the RPE mosaic in eyes with retinal disease," Invest. Ophthalmol. Vis. Sci. **48**(5), 2297–2303 (2007).
11. J. I. W. Morgan, A. Dubra, R. Wolfe, W. H. Merigan, and D. R. Williams, "In Vivo Autofluorescence Imaging of the Human and Macaque Retinal Pigment Epithelial Cell Mosaic," Invest. Ophthalmol. Vis. Sci. **50**(3), 1350–1359 (2008).
12. D. Scoles, Y. N. Sulai, and A. Dubra, "In vivo dark-field imaging of the retinal pigment epithelium cell mosaic," Biomed. Opt. Express **4**(9), 1710–1723 (2013).
13. T. Y. P. Chui, Z. Y. Zhong, and S. A. Burns, "The relationship between peripapillary crescent and axial length: Implications for differential eye growth," Vision Res. **51**(19), 2132–2138 (2011).
14. O. P. Kocaoglu, B. Cense, R. S. Jonnal, Q. Wang, S. Y. Lee, W. H. Gao, and D. T. Miller, "Imaging retinal nerve fiber bundles using optical coherence tomography with adaptive optics," Vision Res. **51**(16), 1835–1844 (2011).
15. G. Huang, X. Qi, T. Y. Chui, Z. Zhong, and S. A. Burns, "A clinical planning module for adaptive optics SLO imaging," Optometry and Vision Science: Official Publication of the American Academy of Optometry. **89**, 593–601 (2012).
16. Z. Y. Zhong, B. L. Petrig, X. F. Qi, and S. A. Burns, "In vivo measurement of erythrocyte velocity and retinal blood flow using adaptive optics scanning laser ophthalmoscopy," Opt. Express **16**(17), 12746–12756 (2008).
17. Z. Y. Zhong, H. X. Song, T. Y. P. Chui, B. L. Petrig, and S. A. Burns, "Noninvasive Measurements and Analysis of Blood Velocity Profiles in Human Retinal Vessels," Invest. Ophthalmol. Vis. Sci. **52**(7), 4151–4157 (2011).
18. T. Y. P. Chui, D. A. Vannasdale, and S. A. Burns, "The use of forward scatter to improve retinal vascular imaging with an adaptive optics scanning laser ophthalmoscope," Biomed. Opt. Express **3**(10), 2537–2549 (2012).
19. P. Bedggood and A. Metha, "Direct visualization and characterization of erythrocyte flow in human retinal capillaries," Biomed. Opt. Express **3**(12), 3264–3277 (2012).
20. Z. Popovic, P. Knutsson, J. Thaung, M. Owner-Petersen, and J. Sjöstrand, "Noninvasive Imaging of Human Foveal Capillary Network Using Dual-Conjugate Adaptive Optics," Invest. Ophthalmol. Vis. Sci. **52**(5), 2649–2655 (2011).
21. T. Y. P. Chui, Z. Y. Zhong, H. X. Song, and S. A. Burns, "Foveal Avascular Zone and Its Relationship to Foveal Pit Shape," Optom. Vis. Sci. **89**(5), 602–610 (2012).
22. J. Tam, K. P. Dhamdhere, P. Tiruveedhula, S. Manzanera, S. Barez, M. A. Bearse, Jr., A. J. Adams, and A. Roorda, "Disruption of the Retinal Parafoveal Capillary Network in Type 2 Diabetes before the Onset of Diabetic Retinopathy," Invest. Ophthalmol. Vis. Sci. **52**(12), 9257–9266 (2011).
23. J. Tam and A. Roorda, "Speed quantification and tracking of moving objects in adaptive optics scanning laser ophthalmoscopy," J. Biomed. Opt. **16**(3), 036002 (2011).
24. Q. Wang, O. P. Kocaoglu, B. Cense, J. Bruestle, R. S. Jonnal, W. H. Gao, and D. T. Miller, "Imaging Retinal Capillaries Using Ultrahigh-Resolution Optical Coherence Tomography and Adaptive Optics," Invest. Ophthalmol. Vis. Sci. **52**(9), 6292–6299 (2011).
25. J. Tam, K. P. Dhamdhere, P. Tiruveedhula, B. J. Lujan, R. N. Johnson, M. A. Bearse, Jr., A. J. Adams, and A. Roorda, "Subclinical Capillary Changes in Non-Proliferative Diabetic Retinopathy," Optom. Vis. Sci. **89**(5), E692–E703 (2012).
26. G. G. Deák and U. Schmidt-Erfurth, "Imaging of the Parafoveal Capillary Network in Diabetes," Curr. Diab. Rep. **13**(4), 469–475 (2013).
27. M. Lombardo, M. Parravano, S. Serrao, P. Ducoli, M. Stirpe, and G. Lombardo, "Analysis of retinal capillaries in patients with type 1 diabetes and nonproliferative diabetic retinopathy using adaptive optics imaging," Retina **33**(8), 1630–1639 (2013).
28. T. Y. Chui, T. J. Gast, and S. A. Burns, "Imaging of vascular wall fine structure in the human retina using adaptive optics scanning laser ophthalmoscopy," Invest. Ophthalmol. Vis. Sci. **54**(10), 7115–7124 (2013).
29. J. H. Kempen, B. J. O'Colmain, M. C. Leske, S. M. Haffner, R. Klein, S. E. Moss, H. R. Taylor, R. F. Hamman, S. K. West, J. J. Wang, N. G. Congdon, D. S. Friedman, and Eye Diseases Prevalence Research Group, "The prevalence of diabetic retinopathy among adults in the United States," Arch. Ophthalmol. **122**(4), 552–563 (2004).
30. N. R. Burrows, I. A. Hora, Y. F. Li, and J. B. Saaddine, "Self-Reported Visual Impairment Among Persons With Diagnosed Diabetes-United States, 1997-2010 (Reprinted from MMWR, vol 60, pg 1549-1553, 2011)," JAMA **307**, 25–27 (2012).
31. X. Z. Zhang, J. B. Saaddine, C. F. Chou, M. F. Cotch, Y. J. Cheng, L. S. Geiss, E. W. Gregg, A. L. Albright, B. E. K. Klein, and R. Klein, "Prevalence of Diabetic Retinopathy in the United States, 2005-2008," JAMA **304**(6), 649–656 (2010).
32. A. Zambelli-Weiner, J. E. Crews, and D. S. Friedman, "Disparities in Adult Vision Health in the United States," Am. J. Ophthalmol. **154**(6 Suppl), S23–S30 (2012).
33. M. K. Ikram, C. Y. Cheung, M. Lorenzi, R. Klein, T. L. Z. Jones, T. Y. Wong, and N. J. W. Retinal; NIH/JDRF Workshop on Retinal Biomarker for Diabetes Group, "Retinal Vascular Caliber as a Biomarker for Diabetes Microvascular Complications," Diabetes Care **36**(3), 750–759 (2013).

#200935 - $15.00 USD Received 15 Jan 2014; revised 15 Jan 2014; accepted 21 Feb 2014; published 27 Feb 2014

34. T. J. Wolfensberger and Z. J. Gregor, "Macular Edema - Rationale for Therapy," in *Macular Edema: A Practical Approach*, G. Coscas, J. CunhaVaz, A. Loewenstein, and G. Soubrane, eds. (2010), pp. 49–58.
35. G. de Venecia, M. Davis, and R. Engerman, "Clinicopathologic correlations in diabetic retinopathy. I. Histology and fluorescein angiography of microaneurysms," Arch. Ophthalmol. **94**(10), 1766–1773 (1976).
36. S. Scholl, J. Kirchhof, and A. J. Augustin, "Pathophysiology of Macular Edema," Ophthalmologica **224**(Suppl 1), 8–15 (2010).
37. A. Garner, "Histopathology of diabetic retinopathy in man," Eye (Lond.) **7**(2), 250–253 (1993).
38. N. Bhagat, R. A. Grigorian, A. Tutela, and M. A. Zarbin, "Diabetic Macular Edema: Pathogenesis and Treatment," Surv. Ophthalmol. **54**(1), 1–32 (2009).
39. D. A. Antonetti, R. Klein, and T. W. Gardner, "Diabetic Retinopathy," N. Engl. J. Med. **366**(13), 1227–1239 (2012).
40. D. R. S. R. Group; The Diabetic Retinopathy Study Research Group, "Preliminary report on effects of photocoagulation therapy," Am. J. Ophthalmol. **81**(4), 383–396 (1976).
41. A. E. Elsner, S. A. Burns, J. J. Weiter, and F. C. Delori, "Infrared imaging of sub-retinal structures in the human ocular fundus," Vision Res. **36**(1), 191–205 (1996).
42. T. Y. P. Chui, T. J. Gast, and S. A. Burns, "Imaging of Vascular Wall Fine Structure in the Human Retina Using Adaptive Optics Scanning Laser Ophthalmoscopy," Invest. Ophthalmol. Vis. Sci. **54**(10), 7115–7124 (2013).
43. R. D. Ferguson, Z. Y. Zhong, D. X. Hammer, M. Mujat, A. H. Patel, C. Deng, W. Y. Zou, and S. A. Burns, "Adaptive optics scanning laser ophthalmoscope with integrated wide-field retinal imaging and tracking," J. Opt. Soc. Am. A **27**, 265–277 (2010).
44. W. Zou, X. Qi, and S. A. Burns, "Wavefront-aberration sorting and correction for a dual-deformable-mirror adaptive-optics system," Opt. Lett. **33**(22), 2602–2604 (2008).
45. W. Y. Zou, X. F. Qi, and S. A. Burns, "Woofer-tweeter adaptive optics scanning laser ophthalmoscopic imaging based on Lagrange-multiplier damped least-squares algorithm," Biomed. Opt. Express **2**(7), 1986–2004 (2011).
46. A. E. Elsner, Q. Zhou, F. Beck, P. E. Tornambe, S. A. Burns, J. J. Weiter, and A. W. Dreher, "Detecting AMD with Multiply Scattered Light Tomography," Int. Ophthalmol. **23**(4/6), 245–250 (2001).
47. D. R. Abrahamson, "Recent Studies On The Structure And Pathology Of Basement Membranes," J. Pathol. **149**(4), 257–278 (1986).
48. Q. D. Nguyen, D. M. Brown, D. M. Marcus, D. S. Boyer, S. Patel, L. Feiner, A. Gibson, J. Sy, A. C. Rundle, J. J. Hopkins, R. G. Rubio, J. S. Ehrlich, and RISE and RIDE Research Group, "Ranibizumab for Diabetic Macular Edema: Results from 2 Phase III Randomized Trials: RISE and RIDE," Ophthalmology **119**(4), 789–801 (2012).
49. M. Al-Latayfeh, P. S. Silva, J. K. Sun, and L. P. Aiello, "Antiangiogenic Therapy for Ischemic Retinopathies," Cold Spring Harbor Perspectives in Medicine **2** (2012).
50. L. An, J. Qin, and R. K. Wang, "Ultrahigh sensitive optical microangiography for in vivo imaging of microcirculations within human skin tissue beds," Opt. Express **18**(8), 8220–8228 (2010).
51. J. Fingler, R. J. Zawadzki, J. S. Werner, D. Schwartz, and S. E. Fraser, "Volumetric microvascular imaging of human retina using optical coherence tomography with a novel motion contrast technique," Opt. Express **17**(24), 22190–22200 (2009).
52. L. An and R. K. Wang, "In vivo volumetric imaging of vascular perfusion within human retina and choroids with optical micro-angiography," Opt. Express **16**(15), 11438–11452 (2008).
53. S. Makita, F. Jaillon, M. Yamanari, M. Miura, and Y. Yasuno, "Comprehensive in vivo micro-vascular imaging of the human eye by dual-beam-scan Doppler optical coherence angiography," Opt. Express **19**(2), 1271–1283 (2011).
54. C. C. Bailey, J. M. Sparrow, R. H. B. Grey, and H. Cheng, "The National Diabetic Retinopathy Laser Treatment Audit. I. Maculopathy," Eye (Lond.) **12**(1), 69–76 (1998).
55. Early Treatment Diabetic Retinopathy Study Research Group, "Grading Diabetic Retinopathy from Stereoscopic Color Fundus Photographs--An Extension of the Modified Airlie House Classification. ETDRS Report Number 10," Ophthalmology **98**(5 Suppl), 786–806 (1991).
56. D. J. Browning, M. M. Altaweel, N. M. Bressler, S. B. Bressler, and I. U. Scott; Diabetic Retinopathy Clinical Research Network, "Diabetic Macular Edema: What Is Focal and What Is Diffuse?" Am. J. Ophthalmol. **146**(5), 649–655 (2008).

1. Introduction

Retinal imaging techniques have undergone rapid and significant changes in recent years. The use of adaptive optics has allowed precise measurements of many cell types in the retina, including photoreceptors [1–9], retinal pigment epithelial (RPE) [10–13] cells, ganglion cell axon bundles [14, 15], and erythrocytes [16–19]. Correcting the wavefront aberrations has also allowed imaging of capillaries at high resolution; increasing contrast and allowing detailed imaging of the perifoveal capillary network [18, 20–24]. The most sensitive of these cellular techniques have usually used confocal imaging, including the use of adaptive optics with OCT. Adaptive optics retinal imaging has been used to study diabetic retinal changes at high magnification [22, 25–27]. [22, 25] Tam and colleagues [22, 25] showed that the

#200935 - $15.00 USD Received 15 Jan 2014; revised 15 Jan 2014; accepted 21 Feb 2014; published 27 Feb 2014

capillary network can be quantified using motion contrast techniques and that it was changing early in diabetes, and Lombardo and colleagues [27] showed capillary diameter changes using a flood illuminated AO system. However confocal AO imaging while producing high contrast and allowing excellent mapping using motion contrast procedures, does not always produce the best structural images of the blood vessels [18]. Flood illuminated AO imaging can show the capillaries and allow quantification [27] but produces relatively low contrasts and is less useful for mapping blood flow. Recently, we have reported that imaging techniques sensitive to lateral scatter can be highly effective for imaging the retinal vasculature [18, 28], and this approach has also been useful in measuring RPE cells [12]. However, to date there have not been applications of this approach to studying retinal vascular diseases [27]. Increasing the proportion of lateral scatter in the image by varying the size and position of the confocal aperture relative to the optical axis was investigated in the current paper applying AOSLO imaging to cellular and vascular structures in mild to moderate non-proliferative diabetic retinopathy.

Diabetic retinopathy (DR) and diabetic macular edema (DME) are the most common causes of blindness in the working age population in the U.S [29, 30]. There are large differences in DR among individuals as well as among different ethnic groups within the U.S [31, 32]. Since the eye also could be a potential biomarker for systemic changes related to diabetes [33], improved retinal imaging is of great significance. The spectrum of neurovascular damage is a consequence of a failure of glycemic control, with consequent microvascular damage and resulting hypoxia [34–39]. Diabetic retinal vascular abnormalities seen in early to moderate NPDR include pericyte loss, basement membrane thickening, arteriole wall thickening, and microaneurysm formation. Some later stages include more extensive retinal vascular remodeling, with important clinical changes such as intraretinal microvascular abnormalities (IRMA) and capillary nonperfusion being potentially difficult to detect by clinical examination. Additionally in DME, fluid accumulates in the retina from leakage through the inner or outer blood retinal barriers, usually visible as leakage on fluorescein angiography (FA) and clinically seen as retinal thickening. Hard exudates, which are the residual protein and lipids from retinal vascular leakage provide one of the more evident clinical signs of DME. As DR progresses further, neovascularization of the optic disk (NVD) as well as neovascularization elsewhere (NVE) can occur [40]. These signs of diabetic retinopathy, the hard exudates, NVD and NVE, are quite evident using traditional imaging techniques. However, the earlier vascular changes such as IRMA and capillary nonperfusion [22, 35–37, 39] are not always evident clinically. With the development of novel therapies and interventions for diabetic control, there is a growing importance for monitoring the early stages of diabetic retinopathy [33]. We investigated the ability of adaptive optics retinal imaging with different degrees of confocality to detect microvascular changes in a cohort of diabetic subjects with mild to moderate NPDR.

Certain microvascular changes are not readily visible with the wide-field imaging that is in general clinical use. However, by using near infrared light to improve retinal penetration [41], along with laser scanning and a confocal aperture to control unwanted scattered light [18, 28], retinal microvascular structures can be imaged at high contrast and high resolution by correcting for each subject's individual optics. For retinal vessels that are perfused, the flow of erythrocytes and other cells can be imaged over time [16, 17, 23] to provide perfusion maps [21, 23]. The perfusion maps allow us to directly evaluate whether capillaries have intact flow without requiring a contrast agent such as sodium fluorescein. These two types of images, the structural images, obtained based on reflectance, and the perfusion map, were examined to test whether the more clinically advanced microvascular changes such as capillary closure and IRMA, are seen in mild to moderate NPDR. Additionally, the image sets were utilized to quantify the wall to lumen ratio of small retinal arterioles (15 to 55 μm) and the diameter of foveal capillaries in this diabetic population compared to appropriate nondiabetic controls.

#200935 - $15.00 USD Received 15 Jan 2014; revised 15 Jan 2014; accepted 21 Feb 2014; published 27 Feb 2014

2. Methods

2.1. Subjects

A series of seven diabetic subjects were imaged. Subjects were recruited from the Indiana University School of Optometry or the Department of Ophthalmology at the Indiana University School of Medicine for testing in Bloomington, Indiana. Prior to imaging, these subjects were graded by a retinal specialist ophthalmologist (A-D.T.P) as having mild to moderate nonproliferative diabetic retinopathy (NDPR) based on the Early Treatment Diabetic Retinopathy Study staging criteria (Table 1). Six of the seven subjects were Type 1 diabetics; the last (D07) was Type 2. Results were compared to control subjects. For measurements of capillary diameter, we used a set of seven healthy control subjects approximately matched in age. For arteriolar wall to lumen ratio comparisons, our technique requires slightly larger blood vessels than the capillaries [42]. For this comparison we used a different group of eight normotensive control subjects. The study was approved by the Indiana University Institutional Review Board and adheres to the tenets set forth in the Declaration of Helsinki and the Health Insurance Portability and Accountability Act regulations. Written informed consent was obtained from all subjects. The control subjects were age-, gender-, and declared ethnicity-status matched, with 3 females in each group. Mean age was 44 ± 6.6 years for the diabetics and 48 ± 8.2 years for the capillary controls and 43 ± 13 years for the normotensive controls, with no age difference between groups ($p>0.05$). All subjects had a comprehensive ophthalmic examination prior to diagnostic testing. All diabetic subjects had chronic hemoglobin A1c greater than 8.0, a clinical diagnosis of mild or moderate NPDR, and no other retinal disease. The control subjects did not have diabetes or other retinal disease. Each subject participated for approximately 1 hour, not including recruitment, consent, and explanation of the data, and travel.

Table 1. Subject information. M: male. F: female. HbA1c: Hemoglobin A1c. CD: capillary diameter. WLR: average wall to lumen ratio for subject.

Subject No.	Age (Year)	Gender	NPDR	HbA1c	Duration (Year)	CD	WLR
D 01	31	M	Moderate	9	22	5.6	0.58
D 02	50	M	Mild	8.1	21	7.7	0.48
D 03	47	F	Mild	9.2	20	8.0	0.82
D 04	47	F	Mild	8.7	16	9.0	2.4
D 05	39	F	Mild	8.3	10	6.5	0.38
D 06	45	M	Mild	9.1	25	8.8	1.7
D 07	48	M	Moderate	9.1	6	6.9	0.64

2.2. Imaging

Infrared SLO fundus imaging and SDOCT imaging were performed first (Figs. 1 and 2, panels A and B) (Spectralis, Heidelberg Engineering, Heidelberg, Germany). This clinical imaging localized retinal areas in the diabetic subjects for further study with the AOSLO, and provided cross-sectional views of retinal reflectivity and thickness maps that could then be related to the high resolution AOSLO imaging [15]. A 20 by 15 deg raster scan centered at the fovea consisting of 144 horizontal optical b-scans was obtained in each subject. The macula was densely sampled to obtain comparison images of small structures, with a separation between each b-scan acquisition of 30 microns. The axial and lateral resolutions of the SDOCT were 7 and 14 microns, respectively. In addition, each subject had measurement of axial lengths using the IOL Master (Carl Zeiss Meditec, Carlsbad, CA).

AOSLO imaging was performed using the Indiana AOSLO [43]. This system uses a woofer tweeter wavefront control system [44, 45] to provide *en face*, high-resolution images of retinal structures, with the capability of focusing on superficial or deeper retinal layers. Images were obtained at 28 Hz frame and 15 kHz line rates, typically 100 consecutive images were digitized at each retinal location for later processing. Template images were

#200935 - $15.00 USD Received 15 Jan 2014; revised 15 Jan 2014; accepted 21 Feb 2014; published 27 Feb 2014

automatically selected from each video segment, and then other frames from the same retinal region were aligned to the template video frame to create video sequences with eye movements removed. To compare diabetic eyes to normal eyes we used two types of images computed from the aligned video data. First, structural images were computed from the averages of the reflected light (Figs. 1 and 2, panel C); second, perfusion maps of the retinal vasculature were computed from the variance of reflectivity over time [21].

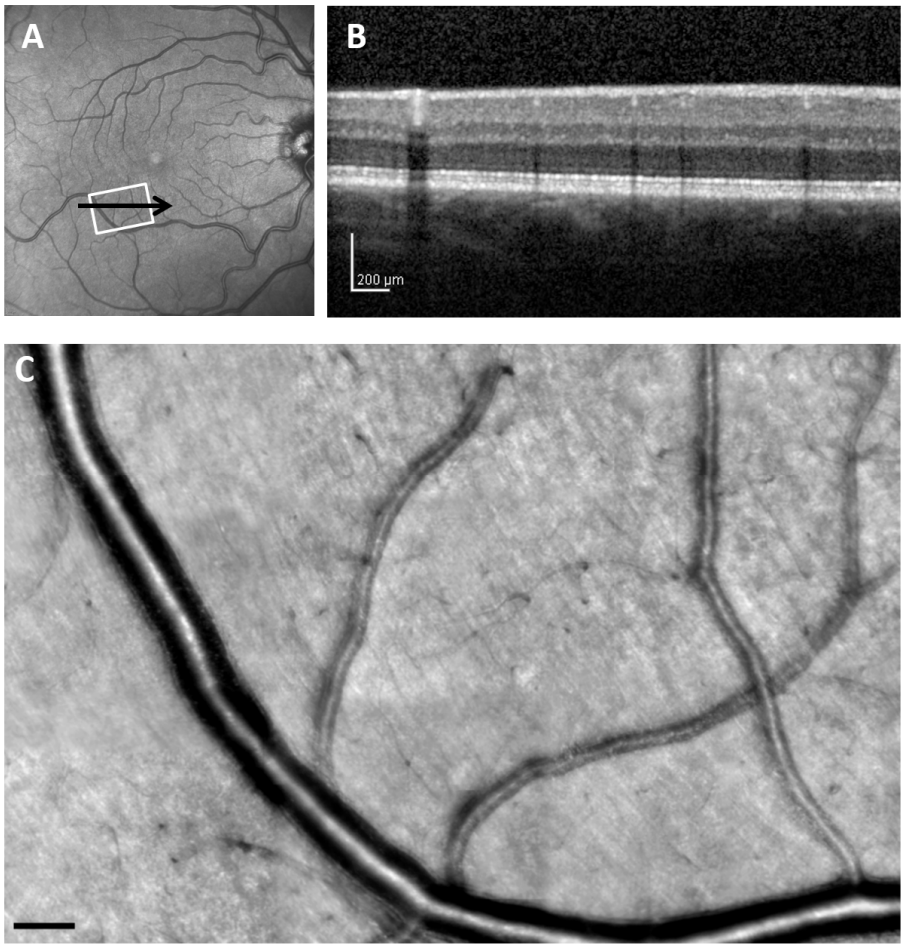

Fig. 1. Retinal images from 35-year-old control subject (C 01), comparing a wide-field SLO en-face image, SDOCT cross section, and AOSLO high resolution montage. (**A**), 30 x 30 deg. wide-field SLO en-face image showing the region of interest. (**B**), SDOCT cross section, with the location as indicated by the black arrow in A. (**C**), Montage of AOSLO reflectance images, corresponding to the white rectangle in A. Scale bar = 100 µm.

Each subject underwent a standard imaging protocol, plus a directed portion where imaging was concentrated on a region of interest that was identified from the wide field imaging. For the standard imaging protocol, the AOSLO was first focused on the foveal photoreceptor layer, which typically provides a bright target for focusing. A strip of retina was imaged using a relatively small confocal aperture (2x the Airy disc diameter) to enhance the contrast of light reflected from the retina, sampling from the fovea to 12 degrees temporally. The regions of interest selected from the SDOCT with the corresponding SLO images were then used with a clinical planning module to target specific locations moving

#200935 - $15.00 USD Received 15 Jan 2014; revised 15 Jan 2014; accepted 21 Feb 2014; published 27 Feb 2014

laterally away from fixation [15] and the photoreceptor layer in this region was imaged (Fig. 3(A)). The AOSLO confocal aperture

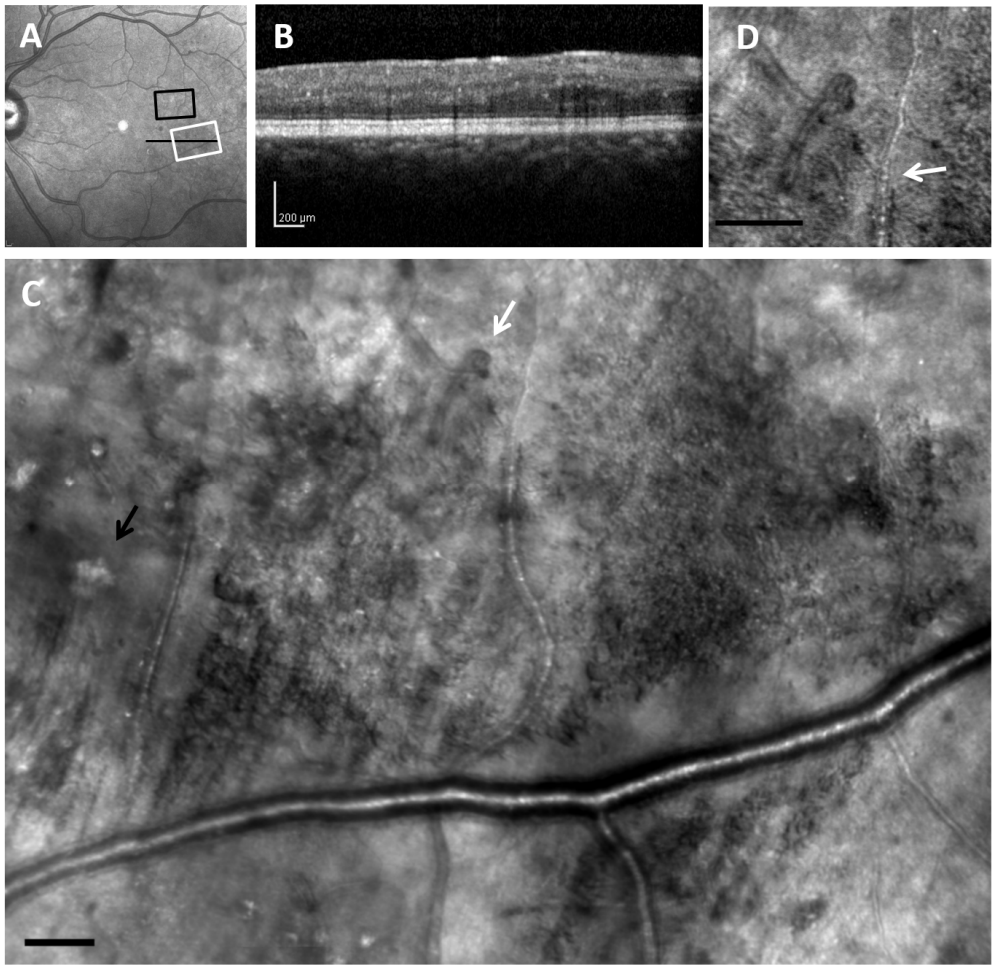

Fig. 2. Retinal images from 31-year-old diabetic subject (D 01) with moderate NPDR. (**A**), 30 x 30 deg wide-field SLO en-face image. (**B**), SDOCT cross section, with the location as indicated by the black arrow in A, demonstrating the lack of visible edema or hard exudate. (**C**), Montage of AOSLO reflectance images, corresponding to the white rectangle in A, showing diffuse capillary remodeling and vessel loops (white arrow), vessel lumen changes, and hard exudates (black arrow). (**D**). Blow up from region of arrow showing a vessel loop as well as changes in small blood vessel wall appearance over space (white arrow). Scale bar = 100 µm.

was then increased in size to 10x the Airy disc diameter to allow more scattered light to be sampled. This change in confocal aperture size improved detection of the moving erythrocytes within the retinal vessels and then the same region of the retina was imaged again (Fig. 3(B)). The depth of focus changed from roughly 70 microns to more than 120 microns. For these images the AOSLO was focused at a retinal depth above the photoreceptors where capillaries were clearly visualized (approximately the inner-nuclear layer). Thus, two sets of matching image data, using the smaller and larger confocal apertures, and focused on different retinal layers were produced. Montages of approximately 4 by 3 deg. were produced at each targeted region following the imaging session, video sequences were analyzed, and average images as well as perfusion maps were constructed [21]. Video

#200935 - $15.00 USD Received 15 Jan 2014; revised 15 Jan 2014; accepted 21 Feb 2014; published 27 Feb 2014

sequences were generated from registered images to provide movies to determine blood perfusion (Fig. 3(B), Media 1).

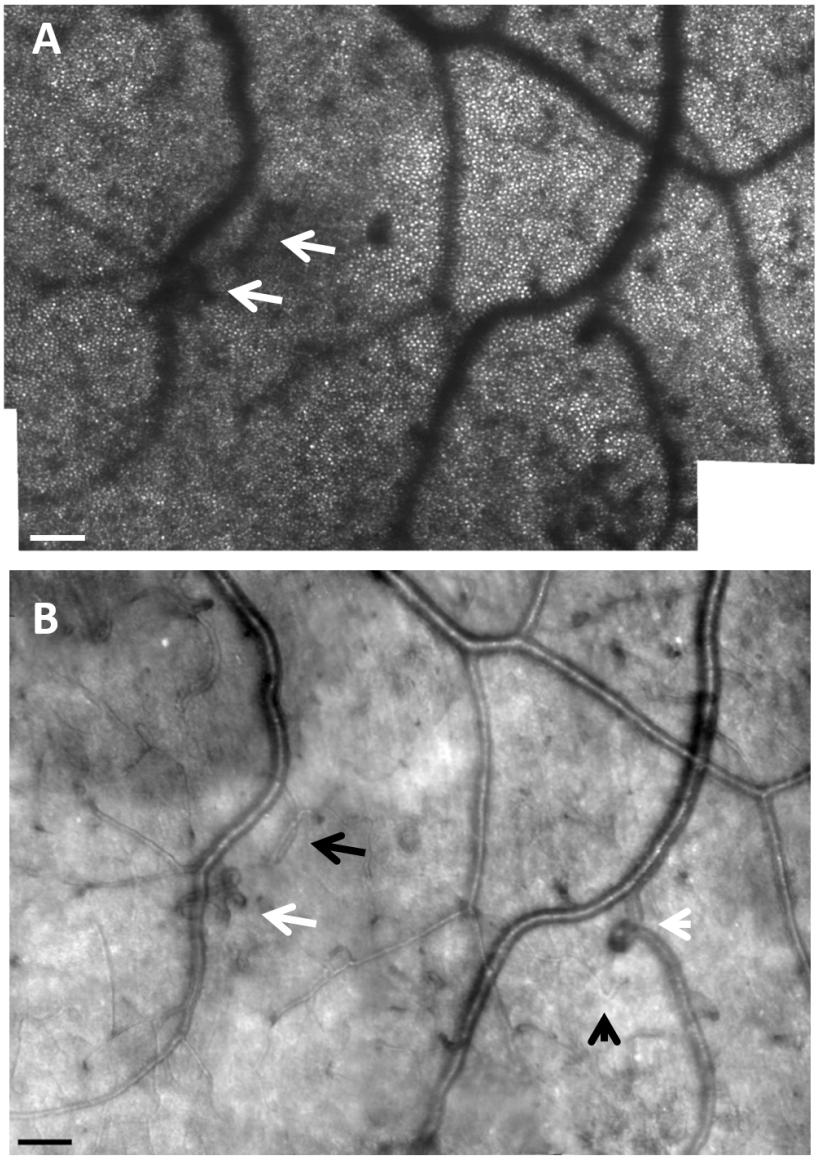

Fig. 3. AOSLO montage from the same subject (D 01) in Fig. 2, sampled from a different retinal location (black box in Fig. 2(A)). (**A**), The appearance of the photoreceptor layer beneath the retinal microvascular changes over space and are often darker (arrows) under regions of vascular remodeling, but not always, (note the top left region of the images to the right of the letters). (**B**). Numerous vessel abnormalities are visible, in particular capillary loops (long white arrow, Media 1), vessel doubling (long black arrow), vessel loop (short white arrow), and non-perfused / ghost capillary (short black arrow, Media 2). Scale bar = 100 μm.

2.3. Vascular measurements

The large aperture imaging allows us to measure vessel sizes and arteriole wall thickness. For this study we measured the wall to lumen ratio for arterioles between 15 and 55 microns in size. Measurements were made on one to three arterioles per subject within the specified size

#200935 - $15.00 USD Received 15 Jan 2014; revised 15 Jan 2014; accepted 21 Feb 2014; published 27 Feb 2014

range. Arterioles were discriminated from venules based on both the direction of motion within the vessels and with reference to the wide field SLO images. We determined the lumen based on the ability to see motion of cells on the video, and the wall as a region distinctly part of the vessel but without moving cells. We then computed the wall to lumen ratio from these two components. This was not possible for capillaries because it was not always possible to image capillary walls (Fig. 2(D), arrow, see ref [28].). Thus, to compare capillary diameters we computed the total diameter of capillaries selected from near the edge of the foveal avascular zone. The distance of the measured capillaries from the fixation location for patients and controls was determined by having the subject fixate a specific region on the raster, which was visible to the subject. For each data point, manual measurements were made five times along a short vessel segment using the Adobe Photoshop CS5 (Adobe Systems, San Jose, CA) measurement tool, drawing a line orthogonal to the blood vessel each time. In pilot experiments, we investigate the effect of grader on measurements by having two different graders measure 21 arterioles. Comparing grader measurements gave an intraclass correlation of 0.99, and so for the data reported we used results from a single grader. The mean wall to lumen ratios and the perifoveal capillary diameters for diabetic versus control subjects were compared on a per subject basis with repeat measures ANOVA. Distances from fixation to the measured capillaries were compared using a t-test. We also compared measurements between graders and found that the diameter measurements were reproducible to within 5% (data not shown).

3. Results

Retinal microvascular changes and spatially related photoreceptor image changes were evident for all diabetic subjects in all AOSLO image types. For the diabetic subjects, the AOSLO photoreceptor layer images showed regions of bright cones and dark regions (Fig. 3(A)). These dark regions typically matched areas of overlying vascular remodeling (Fig. 3(B)) as well as areas of overlying retinal edematous changes (Fig. 4(E)) although there were not always darkened or abnormal appearing photoreceptors below areas of retinal remodeling (upper left corner of Fig. 3(A) and 3(B)) . In some cases these dark regions were apparent even with relatively small changes such as a haziness of the inner retinal layer images (upper arrow in Fig. 3(A) and 3(B)).

Remodeled retinal capillaries and microaneurysms were clearly visualized in diabetic subjects, particularly with the AOSLO focused on the inner retinal layers and using the larger confocal aperture (Figs. 2(C), 3(B), 4(C), and 5(A)-5(E)) to capture more of the light scattered from the vasculature [18]. The apparent differences from the control subjects included the presence of irregular branching of retinal blood vessels, the presence of shunt vessels, capillary sprouts, and variable diameter of vessel branches as well as the well documented irregularities of retinal layers apparent in SDOCT images (compare Fig. 1, 2, and 4). Microaneurysms of varying shape with blood flow ranging from occlusion to rapid spiraling flow were observed. In both mild and moderate NPDR, capillary dilation and capillary tortuosity were prevalent. Because the morphology of these changes were so variable no clear grouping was evident, however there were numerous capillary sprouts, an early stage of IRMA, as well as “hairpin” or “duplicated” capillaries (Figs. 3(B) and Media 1).

Blood flow patterns were variable, sometimes including local stasis (Media 2) and microaneurysms (Media 4). For the capillary observed without flow (black arrow Fig. 3 and Media 2), the lack of flow was observed for a total period of 2 min. In some instances, regions of retina that did not appear distorted on clinical SDOCT b-scans images were found to be abnormal on AOSLO imaging. These abnormalities included non-perfused capillaries as well as irregularly shaped capillaries, consistent with retinal ischemia (Fig. 2(C) and Media 2 and Media 5).

#200935 - $15.00 USD Received 15 Jan 2014; revised 15 Jan 2014; accepted 21 Feb 2014; published 27 Feb 2014

Hard exudates were clearly visualized, and were more extensive than might be expected from the clinical grade or the wide-field SLO and SDOCT images (Fig. 2 and Figs. 4(A) and 4(B)). The AOSLO, showed hard exudates with sizes less than 10 microns, too small to be readily detected by SDOCT (Fig. 4(C)).

Microaneurysms were typically seen in the diabetic subjects, but were not seen in the control subjects (Fig. 5(A)-5(E)). Microaneurysms differed in the degree of dilation and appearance of the nearby capillaries, some of which had darker walls and/or larger lumens than other nearby capillaries (Fig. 5). In addition, the microaneurysms varied in that some had blood flow throughout the cross-section of the microaneurysm while others had only a central thread of visible blood flow, and some were intermediate (Fig. 5(B)-5(E)). The large confocal aperture allowed determining the motion contrast images using less than 3 sec. of imaging per location.

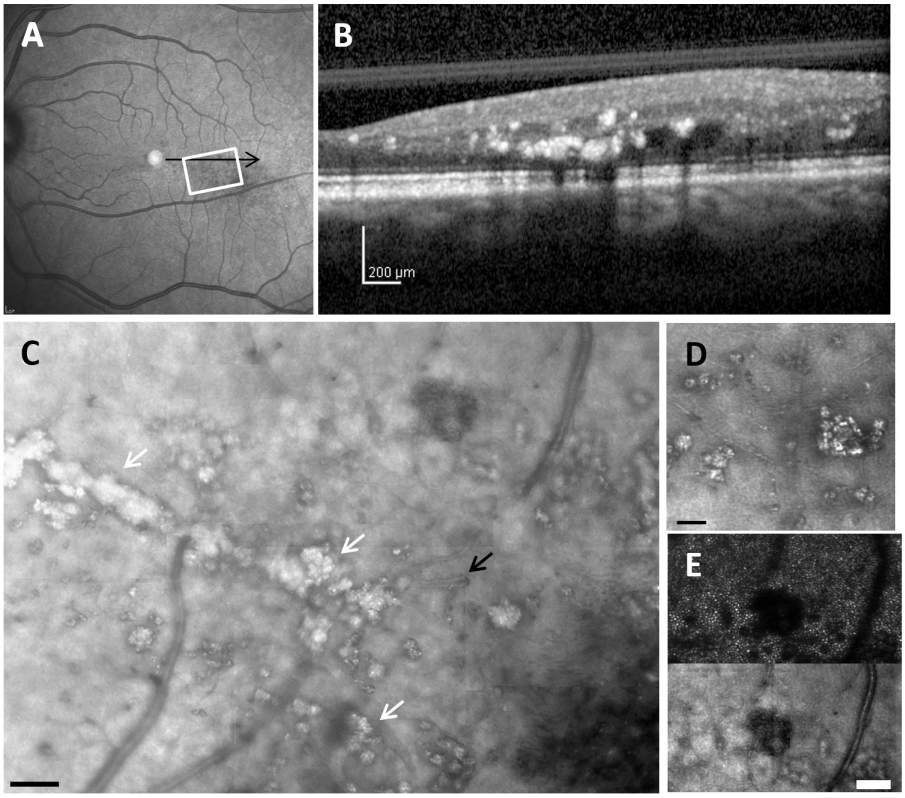

Fig. 4. Retinal images from 47-year-old diabetic subject with mild NPDR and clinically significant macular edema. (**A**), 30 x 30 deg wide field SLO image showing hard exudates and edema. (**B**), SDOCT cross section, with the location as indicated by the black arrow in A, showing extensive hard exudates and intraretinal fluid. (**C**), montage of AOSLO reflectance image also showing corresponding extensive hard exudates (white arrows), and in addition surrounding numerous capillary abnormalities including vessel looping (black arrow). The dark region in the lower right corner is a typical appearance of loss of reflectivity due to the accumulation of fluid. Scale bar = 100 µm. (**D**), Enlargement of region of multiple hard exudates, showing sizes as small as 5 µm. (**E**), comparison of a region of edema as indicated by cysts in the inner retina, top- imaging focused on photoreceptors using a 2x Airy disc aperture, bottom- same region with offset aperture focused on blood vessels. For C scale bar = 100 µm, for D and E Scale bar = 50 µm.

In addition to these qualitative observations we measured quantitative changes in the blood vessels. For the perifoveal capillaries, the diabetic patients had an average capillary diameter of 8.2 µm (standard deviation (SD 1.1 µm), while the normal subjects had an

#200935 - $15.00 USD Received 15 Jan 2014; revised 15 Jan 2014; accepted 21 Feb 2014; published 27 Feb 2014

average diameter of 6.1 μm (SD of 0.75 μm). This difference between groups was significant (repeat measures ANOVA, $p < 0.01$). These capillaries were measured at or near the edge of the foveal avascular zone and there was no significant difference in distance from fixation for the diabetic (283μm, SD 62μm) and normal subject (309 μm, SD 81μm; $p = 0.5$, t-test). In these measurements, we avoided measuring the obviously dilated capillaries seen in IRMA or feeding microaneurysms and only measured those with seemingly normal architecture. The arterioles used for wall to lumen ratio measurements were primarily sampled during the directed imaging portion of the measurements since our standard locations (at the fovea and along the temporal midline) had few arterioles. For the vessels measured, we obtained a wall to lumen ratio of 0.48 (SD 0.28) in normal subjects and a ratio of 1.1 (SD 0.87) in diabetics. This difference was significant (ANOVA, $p<0.05$).

4. Discussion

We found that we could obtain clear visualization of a wide variety of retinal vascular and non-vascular changes in subjects with mild to moderate NPDR using an AOSLO. By incorporating multiply scattered light into the images i.e. by using the large aperture [46], we were able to clearly see the smallest capillaries and the remodeling of the capillaries that occurred in the diabetic eyes as well as map the capillaries with intact flow using a variance based method [21]. The structural imaging enabled us to image the vascular walls and to quantify increases in the wall to lumen ratio of arterioles and increases in perifoveal capillary diameters in diabetic subjects. These changes were seen not only near microaneurysms (Fig. 6) but more extensively (Figs. 2 and 6). Because we collect video data, we were able to detect capillaries, and also to determine whether they were perfused, which is not possible using vascular imaging techniques that depend primarily on blood flow or dyes to generate contrast. Our results apparently differ somewhat from a recent report [27] that indicates a decrease in capillary lumens in individuals with longer duration diabetes. Both studies have relatively small sample sizes, and there are several important differences. First, we measured total diameter of the capillaries, while Lombardo et al measured the lumens. Also, the reported sizes differ, since the capillary lumens of their diabetic subjects were similar to our control subjects' total diameters. The most likely difference is simply population differences mixed with the choice of vessels to be measured. We used a fixed location near the fovea without marked edema because we noted large capillary to capillary diameter changes in areas with edema and IRMA (for instance Fig. 2(D) shows both narrow and broad capillaries). Additionally, since basement membrane is definitely thickened in the capillaries of diabetics [47], it is possible that capillary diameters are increased while lumens are decreased. The present study was intended to assess our ability to make reliable measurements in diabetic subjects, and only larger, longitudinal studies will clarify the true prognostic value of the measurements

The increase in retinal thickness from the fluid leakage in DME is typically quantified using SDOCT, either over time or compared with normative values from control subjects. Our findings suggest that AOSLO imaging ca provide complementary information because fluid accumulation is readily visualized as darkening of the image, presumably due to increased intraretinal scatter, and hard exudates even of only a few microns in diameter are readily detected. Improvements in detection and quantification are desirable because while anti-VEGF and other anti-inflammatory therapies are successful, there remains a wide range in the success for specific patients and over time for these interventional treatments [48, 49]. A better method of monitoring the effects of treatment may be helpful. While the use of retinal thickness from OCT provides a quantitative metric against which to measure improvement after treatment,

#200935 - $15.00 USD Received 15 Jan 2014; revised 15 Jan 2014; accepted 21 Feb 2014; published 27 Feb 2014

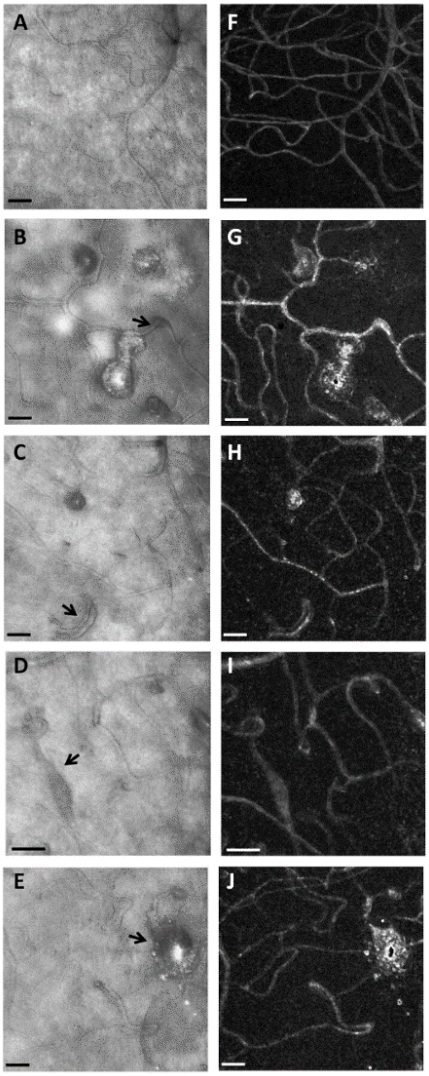

Fig. 5. AOSLO reflectance images (left column, Panels A, B, C, D, and E) and corresponding perfusion maps (right column, Panels F, G, H, I, and J), in a control subject (top row) and 4 diabetic subjects obtained during the directed portion of the imaging session. **A and F**, 49-year-old normal subject, showing relatively uniform capillary network and vessel diameters, except in the lower left corner where the normal low density of capillaries at the foveal center occurs (Media 3). **B and G**, 50-year-old diabetic subject with mild NPDR, showing microaneurysms of varying sizes that differ in the degree of perfusion. These microaneurysms had a wide range of apparent blood flow velocities including stasis (Media 4). **C and H**, Capillary doubling (black arrow) with distinct blood flow in each branch. **D and I**, Dilated capillary with fusiform shape (black arrow). The video (Media 5) shows a pressure wave that occurred at approximately 1 second intervals in the corresponding capillary. **E and J**, Structural image and perfusion map of an unusually large microaneurysm surrounded by dilated capillaries. Scale bars = 50 μm.

this method is made more variable by neural loss and can be normal after microvascular changes have already occurred. Thus, the retinal thickness metric does not report on whether there is an improvement in capillary perfusion, or if an individual already has extensive capillary remodeling and ischemia. The retinal ischemia demonstrated by capillary non-perfusion or remodeling may actually lead to a thinner, not necessarily thicker, retinal

#200935 - $15.00 USD Received 15 Jan 2014; revised 15 Jan 2014; accepted 21 Feb 2014; published 27 Feb 2014

measurement. Furthermore, although the SDOCT provides excellent images of hard exudates, these are not incorporated in a metric based solely on thickness. Additionally, it is often difficult or impossible to detect structurally abnormal or nonperfused intraretinal capillaries clinically, or even with current commercially available diagnostic devices such as SDOCT. While OCT flowmetry techniques hold great promise for delineating the intact vasculature [50–53], the AOSLO approach can image occluded capillaries (Fig. 3(B), Media 2)

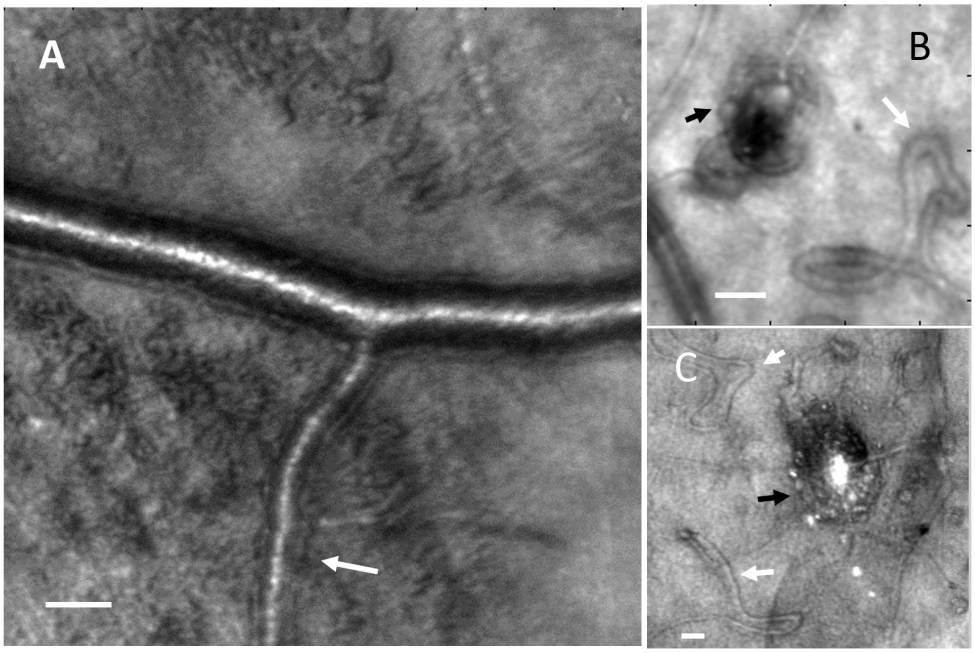

Fig. 6. (**A**). AOSLO reflectance images showing thickened arteriole walls (white arrow) and widespread tissue changes (apparently roughened surface). Panel A is an image from the same region of the subject shown in Fig. 3. Scale bar = 50 μm. **B, C** microaneurysms and capillary remodeling including loops and hairpins. The layering of cells surrounding microaneurysms can be seen (black arrows) as well as capillary remodeling (white arrows). Scale bar = 25 μm.

Our results, together with the results of Tam [22, 25], make a strong case that the current classifications of diabetic retinopathy that are based on lower resolution and lower contrast imaging methods provide insufficient specific information about the status of the retina. Imaging with AO opens the possibility of distinguishing among patients who are undergoing retinal changes that permanently threaten sight. There is a clear demonstration that at least some of the small vessel remodeling is not a fleeting phenomenon, since the capillary changes were repeatable and progressed over 16 months [25]. However, this long term follow-up was of a single case with a classification of severe non-proliferative diabetic retinopathy [25]. The argument could be made that these changes are not necessarily typical of mild or moderate non-proliferative diabetic retinopathy, and might be found only shortly before advancement to proliferative diabetic retinopathy. Also there simply is considerable variability across patients [54]. Thus, we analyzed a broader range of cases with an emphasis on Type 1 diabetes to show that the vessel remodeling is beginning in earlier stages of diabetic retinopathy in some patients, but cannot be detected by the usual clinical instruments. By combining the blood flow based measurement of vascular integrity with the structural imaging enabled by the AOSLO using an offset aperture we also showed that both the capillaries and mid-sized arterioles were also changing in these patients. These results taken together point to some patients having many small changes in the retinal vasculature across the retina, even though these are not apparent on clinical examination.

#200935 - $15.00 USD Received 15 Jan 2014; revised 15 Jan 2014; accepted 21 Feb 2014; published 27 Feb 2014

Further, our results clearly point out significant vessel remodeling in mild to moderate nonproliferative diabetic retinopathy, not limited to capillary dilation. Our results are consistent with both endothelial cell proliferation and also the migration of endothelial cells necessary to provide new blood vessel formation such as the vessel loop in Figs. 2 and 3, i.e. more than bends in thickened capillaries.

This type of imaging applied to the realm of clinical research opens the possibility of improving our understanding of the development of those diabetic retinal changes effecting vision of individuals based on a much more finely graded phenotype. In diabetic retinas, there is an inter-related set of microvascular changes that develop over time [22, 35, 37–39, 55]. Certainly there are distinct patterns or phenotypes seen in clinical populations [54, 56]. Diabetic retinopathy at one extreme shows a purely ischemic diabetic maculopathy with loss of capillaries dominating, similar to the poorly perfused capillary bed seen in Fig. 3. Another pattern of focal edema is leakage dominated by microaneurysms, and at another extreme, a pattern of diffuse macular edema, with a range of intermediate variants similar to Fig. 4. Improved understanding is needed to determine both the patterns of capillary changes which occur over time in different patients and to test whether the changes seen with AOSLO correspond to the clinical classification and whether they are better prognosticators of the eventual clinical outcome [56].

In summary, using large aperture AOSLO imaging has allowed us to visualize directly numerous capillary abnormalities in subjects with mild and moderate NPDR, indicating that pre-neovascular processes are already occurring in some individuals. These observed changes could contribute to the variability in response to treatment in diabetic patients. Thus, these microvascular changes that include extensive blood vessel remodeling, non-perfusion, and vascular leakage resulting in small hard exudates, could hold the key for improved clinical classification of diabetic patients, better understanding of the mechanisms of diabetic retinopathy, and development of more effective therapies through better patient monitoring of pharmacological intervention using this technology.

Acknowledgments

NIH Grants EY004395, EY007624, EY14375, P30EY019008, K23-EY017886, and Indiana Diabetes Translational Research Center

#200935 - $15.00 USD Received 15 Jan 2014; revised 15 Jan 2014; accepted 21 Feb 2014; published 27 Feb 2014